ELSEVIER

Journal of Hazardous Materials B124 (2005) 74–80

Journal of Hazardous Materials

www.elsevier.com/locate/jhazmat

Application of an effective method in predicting breakthrough curves of fixed-bed adsorption onto resin adsorbent

B.C. Pan [a,b,*], F.W. Meng [a], X.Q. Chen [a], B.J. Pan [a], X.T. Li [a], W.M. Zhang [a], X. Zhang [a], J.L. Chen [a,b], Q.X. Zhang [a,b], Y. Sun [c]

[a] *School of the Environment, and State Key Laboratory of Pollution Control and Resources Reuse, Nanjing University, Nanjing 210093, PR China*
[b] *Research Center for Engineering Technology of Organic Pollutant Control and Resources Reuse in Jiangsu Province, Nanjing 210038, PR China*
[c] *School of the Environment, Nanjing University, PR China*

Received 2 November 2004; received in revised form 25 February 2005; accepted 24 March 2005
Available online 21 June 2005

Abstract

Removal of many organic pollutants including phenolic compounds from industrial wastewater can always be achieved by fixed-bed adsorption onto the polymeric resin adsorbent, and the relevant breakthrough curves would provide much valuable information to help to design a fixed-bed adsorption process in field application. In the present study, a model developed based on the constant-pattern wave approach theory and the Freundlich model was adopted to describe the breakthrough curves of phenol and *p*-nitrophenol adsorption onto a macroreticular resin adsorbent NDA-100 from aqueous solution. Column experiments were performed at different conditions to verify the model and the results proved that the model would describe the breakthrough curves well. Effect of the operation parameters on breakthrough curves was also discussed to get helpful information in choosing the adsorption process.

Keywords: Phenol; Fixed-bed adsorption; Breakthrough curve; Mathematical model; Resin adsorbent

1. Introduction

Fixed-bed adsorption process has been widely used to remove many organic pollutants including phenolic compounds from industrial wastewater, and the relevant breakthrough curves for a specific adsorption process are essential when determining the operating parameters such as feed flow rate and aspect ratio [1–6]. Although many models were developed to predict the breakthrough curve, most of them are sophisticated and need many parameters determined by serial independent batch kinetic tests or estimated by suitable correlations [7–12]. Hence, a model without tedious tests or mathematical calculations is needed to predict the breakthrough curve.

In the present study, an effective method based on combining the constant-pattern wave approach theory and the Freundlich model was used to determine the breakthrough curve of a fixed-bed adsorption system. A macroreticular polymeric resin adsorbent NDA-100 was selected as adsorbent for its wide use in theoretical study and field application [13,14], and phenol and *p*-nitrophenol were selected as adsorbates due to their frequent appearance in industrial wastewater [15–17]. The adsorption isotherms of both phenolic compounds onto resin NDA-100 were obtained to help to develop the model. Column experimental results obtained at different test conditions proved the validity of the model well.

2. Model [18,19]

Here, we consider an aqueous solution containing organic pollutant fed to the top of a column packed with resin particles randomly. The governing equation for predicting column dynamics is [20]:

$$\varepsilon\frac{\partial C}{\partial t} + u_0\varepsilon\frac{\partial C}{\partial z} + \rho\frac{\partial q}{\partial t} = 0 \quad (1)$$

* Corresponding author. Tel.: +86 25 83231724; fax: +86 25 83707304.
E-mail address: bcpan@nju.edu.cn (B.C. Pan).

0304-3894/$ – see front matter © 2005 Elsevier B.V. All rights reserved.
doi:10.1016/j.jhazmat.2005.03.052

Nomenclature

a	mass-transfer area per unit volume of the bed (m^2/m^3)
C	phenols concentration in the mobile phase (mmol/L)
C_F	feed phenols concentration in the mobile phase (mmol/L)
C^*	equilibrium phenols concentration in the mobile phase (mmol/L)
d_p	resin particle diameter (m)
D	molecular diffusion coefficient of phenols in water (m^2/h)
K_F	Freundlich model parameter (m^{3n} mol^{1-n}/kg)
K_1	Langmuir model parameter (m^3/mol)
k_L	individual liquid-phase mass-transfer coefficient (m/h)
K_L	overall liquid-phase mass-transfer coefficient (m/h)
K_La	the volumetric coefficients in the liquid-phase (h^{-1})
L	bed height (cm)
L/R	aspect ratio
n	Freundlich model parameter
q_m	Langmuir model parameter (mmol/g)
q	phenols concentration in the stationary phase (mmol/g dry resin)
q^*	phenols concentration in the stationary phase equilibrium with C* (mmol/g dry resin)
q_F	phenols concentration in the stationary phase equilibrium with C_F (mmol/g dry resin)
Q	volumetric flow rate (mL/h)
R	the inside diameter of glass column (cm)
t	time (h)
T	solution temperature (K)
$t_{1/2}$	half time at $x = 1/2$ (h)
u_0	interstitial fluid velocity (cm/h)
μ	carrier fluid viscosity (kg/m h)
u_c	concentration wave velocity (cm/h)
V	the volume of solution (L)
W	the weight of dry resin (g)
x	the normalized effluent concentration, $x = C/C_F$
z	the distance from the inlet of mobile phase (m)
ε	void fraction of bed
ρ	resin bed density (g/L)
ρ_L	carrier fluid density (kg/m^3)
τ	adjusted time (h)
$\tau_{1/2}$	half adjusted time at $x = 1/2$ (h)

where ε is the bed void fraction, t is the contact time, u_0 is the interstitial flow rate, z is the distance from the inlet of the bed, ρ is the bed density, C and q are the adsorbate concentration in the liquid and solid phases, respectively. Eq. (1) is the unsteady-state mass balance for the adsorbate.

The adsorption rate can be described by the linear driving force model in terms of the overall liquid-phase mass-transfer coefficient [21]:

$$\rho\frac{\partial q}{\partial t} = \varepsilon K_L a(C - C^*) \tag{2}$$

where K_L is the overall liquid-phase mass-transfer coefficient, a is the contact area per unit volume of the bed, K_La can be called as the volumetric coefficients in the liquid-phase, and C^* is the liquid-phase concentration in equilibrium. The adsorption isotherm related the liquid- and solid-phase concentrations at equilibrium:

$$C^* = f(q) \quad or \quad q^* = g(C) \tag{3}$$

In the terms of the constant-pattern wave approach theory [22], the waves move at a constant flow velocity, u_c. Then the liquid-phase concentration can be expressed as a unique function of the adjusted time τ, defined as:

$$\tau = t - \frac{z}{u_c} \tag{4}$$

Substituting Eq. (4) into Eq. (1) leads to:

$$\left(1 - \frac{u_0}{u_c}\right)\frac{dC}{d\tau} + \frac{\rho}{\varepsilon}\frac{dq}{d\tau} = 0 \tag{5}$$

which can be integrated as:

$$\int_0^C \left(1 - \frac{u_0}{u_c}\right)\frac{dC}{d\tau} + \int_0^q \frac{\rho}{\varepsilon}\frac{dq}{d\tau} = 0 \quad \text{or}$$

$$\left(1 - \frac{u_0}{u_c}\right)C + \frac{\rho}{\varepsilon}q = 0 \tag{6}$$

Because the boundary condition $q = q_F$ at $C = C_F$ is satisfied all the time, the following equation is also valid:

$$\left(1 - \frac{u_0}{u_c}\right)C_F + \frac{\rho}{\varepsilon}q_F = 0 \tag{7}$$

where C_F is the feed adsorbate concentration in the liquid-phase and q_F is its associated equilibrium concentration in solid-phase.

Combining Eqs. (6) and (7) leads to:

$$\frac{q}{q_F} = \frac{C}{C_F}. \tag{8}$$

This is the keystone for deriving the breakthrough curves of fixed-bed adsorption process. The adsorption rate expressed in terms of the adjusted time is:

$$\rho\frac{dq}{d\tau} = \varepsilon K_L a\left(C - C^*\right) \tag{9}$$

Combining Eqs. (3), (8) and (9), we obtain:

$$\frac{\rho q_F}{C_F}\frac{dC}{d\tau} = \varepsilon K_L a\left[C - f\left(q_F\frac{C}{C_F}\right)\right] \tag{10}$$

This can be rearranged and integrated with the following boundary condition $C = C_{F/2}$ at $\tau = \tau_{1/2}$,

$$\int_{C_{F/2}}^{C} \frac{1}{C - g(q_F C/C_F)} dC = \int_{\tau_{1/2}}^{\tau} \varepsilon K_L a \frac{C_F}{\rho q_F} d\tau \quad (11)$$

where $\tau_{1/2}$ is the adjusted time when the effluent adsorbate concentration reaches half of the feed concentration. Assuming $K_L a$ is constant, Eq. (11) becomes:

$$\tau = \tau_{1/2} + \frac{\rho q_F}{\varepsilon K_L a C_F} \int_{C_{F/2}}^{C} \frac{1}{C - g(q_F C/C_F)} dC. \quad (12)$$

Since $\tau - \tau_{1/2} = (t - (z/u_c)) - (t_{1/2} - (z/u_c)) = t - t_{1/2}$ from Eq. (4), the breakthrough curves at $z = L$ can be calculated by the following equation:

$$t = t_{1/2} + \frac{\rho q_F}{\varepsilon K_L a C_F} \int_{C_{F/2}}^{C} \frac{1}{C - g(q_F C/C_F)} dC. \quad (13)$$

3. Experimental

3.1. Materials

The macroreticular resin adsorbent NDA-100 was provided kindly by Langfang Electrical Resin Co. Ltd., Hebei Province, China. The resin particles were extracted with ethanol for 8 h in a Soxlet apparatus and vacuum desiccated at 325 K to constant weight, followed by storage in a sealed bottle for later use. Physiochemical properties of the adsorbent are presented in Table 1.

Phenol and *p*-nitrophenol used in this study are of analytical grade and were purchased from Shanghai reagent station. Their concentrations in aqueous solution were determined by an UV spectrometer (Heλ10SβUnicam, British) at 270 and 318 nm, respectively.

3.2. Batch adsorption runs

First, 0.250 g resin samples were added to several 250 mL sealed flasks, a 100-mL aqueous solution containing known concentration of phenols was then added into each flask.

Table 1
Physiochemical properties of resin NDA-100 [23]

Matrix structure	Polystyrene
Crosslink density (%)	>40
BET surface area (m^2/g)	721.5
Macropore volume (cm^3/g)	0.36
Mesopore volume (cm^3/g)	0.028
Micropore volume (cm^3/g)	0.42
Particle size d_p (mm)	0.7–0.8
Particle density ρ (g/L)	321.9

Afterwards, the flasks were shaken at 200 rpm and the desired temperature in a G 25 model incubator shaker with thermostat (New Brunswick Scientific Co., Inc.) for 24 h to attain equilibrium. The amounts of phenolic compounds adsorbed by resin particles were calculated by the mass balance relation:

$$q_F = (C_F - C^*) \times \frac{V}{W} \quad (14)$$

where V is the volume of solution, W is the weight of dry resin.

3.3. Column adsorption experiments

Fixed-bed adsorption runs were carried out in glass columns with inside diameter of 1.48, 1.06 and 1.92 cm, respectively, and length of 20 cm. Every column was packed with a water jacket to maintain a desired constant operation temperature. The solution with known contents of phenol or *p*-nitrophenol was fed to the top of the column at a desired flow rate regulated by a constant-speed pump. The effluent samples were collected at intervals and analyzed spectrometrically. The experimental conditions are listed in Table 2.

4. Results and discussion

4.1. Adsorption isotherm

The isotherms of phenol and *p*-nitrophenol onto resin NDA-100 at natural pH (shown in Fig. 1) were described by Langmuir and Freundlich model, respectively.

$$q = \frac{K_1 q_m C}{1 + K_1 C} \quad (15)$$

$$q = K_F C^{1/n} \quad (16)$$

where q_m is the monolayer sorption capacity and K_1 is the Langmuir constant, K_F and n are Freundlich constants.

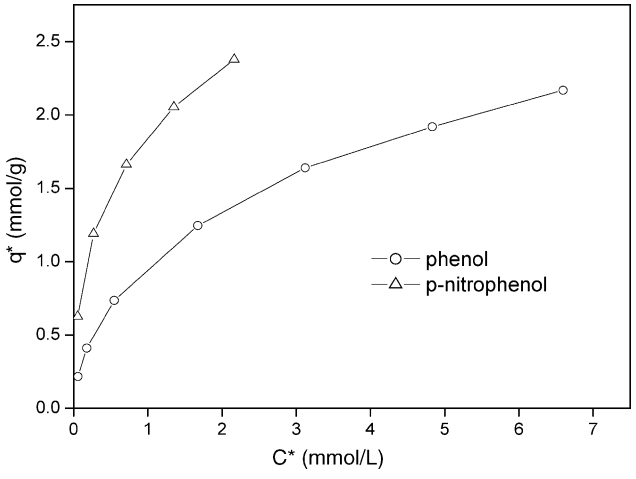

Fig. 1. Adsorption isotherms of phenol and *p*-nitrophenol onto resin NDA-100 at 298 K.

Table 2
Experimental conditions for column tests

Experiment conditions	Phenol									*p*-Nitrophenol		
	Run 1			Run 2		Run 3	Run 4	Run 5		Run 6		
Flow rate (cm/h)	**17.4**	**34.9**	**52.3**	34.9	34.9	34.9	34.9	34.9	34.9	**17.4**	**34.9**	**52.3**
Concentration of feed solution (mmol/L)	5.32	5.32	5.32	**0.53**	**2.13**	5.32	5.32	5.32	5.32	5.32	5.32	5.32
Bed depth (cm)	5.71	5.71	5.71	5.71	5.71	**2.86**	5.71	3.41	11.02	5.71	5.71	5.71
temperature (K)	298	298	298	298	298	298	**313**	298	298	298	298	298
Aspect ratio	3.88	3.88	3.88	3.88	3.88	3.88	3.88	**1.77**	**10.32**	3.88	3.88	3.88
Bed void fraction ε (%)	14.31	14.31	14.31	14.31	14.31	14.31	14.31	14.31	14.31	14.31	14.31	14.31
Bed density ρ (g/L)	321.9	321.9	321.9	321.9	321.9	321.9	321.9	321.9	321.9	321.9	321.9	321.9
$t_{1/2}$ (h)												
Experimental	37.21	18.24	12.11	70.12	33.05	9.15	16.65	18.5	18.1	57.71	27.22	18.19
Calculated	37.43	18.47	12.16	70.64	33.27	9.61	16.87	19.01	18.17	55.69	27.81	18.4
$K_L a$ (h^{-1})	138.7	175.1	232.6	108.5	129.9	163.8	138.1	152.1	137.7	407.4	522.6	630.8

Parameters were determined from non-linear regression of experimental data and the results are shown in Table 3. It can be seen that the Freundlich model gives more satisfactory fit to the experimental results. Additionally, *p*-nitrophenol is more hydrophobic (the water solubility of phenol and *p*-nitrophenol is 9.3 and 1.4 g/100 g H_2O at 298 K, respectively) and loaded on the resin more easily than phenol. The result is consistent with the conclusion in literature that high hydrophobicity was found favorable to the adsorption of organic compounds onto non-polar and moderate polar polymeric adsorbents from aqueous solutions [24].

4.2. Breakthrough dynamics

We combine Eq. (13) with (16) and obtain:

$$t = t_{1/2} + \frac{\rho q_F}{\varepsilon K_L a C_F}\left[\ln 2x - \frac{1}{n-1}\ln\frac{1-x^{n-1}}{1-(2)^{1-n}}\right] \quad (17)$$

where x is the normalized effluent concentration ($x = C/C_F$). The applicability of Eq. (17) is justified by the liner plot as shown in Fig. 2. The value of $t_{1/2}$ and $K_L a$ determined from the intercept and slope of the $[\ln 2x - (1/n-1)\ln(1 - x^{n-1}/1-(2)^{1-n})]$ versus t curve are listed in Table 2.

The experimental and predicted breakthrough curves calculated by Eq. (17) are shown in Fig. 3 and other figures. The results imply the above-described model can predict phenol and *p*-nitrophenol adsorption from aqueous solution on resin NDA-100 satisfactorily. Larger values of $t_{1/2}$ and $K_L a$ for *p*-nitrophenol than phenol may be related to their different adsorption capacity and hydrophobicity.

Table 3
Parameters for Langmuir and Freundlich model

Adsorbate		Freundlich			Langmuir		
	T (K)	K_F	n	R^2	K_1	q_m	R^2
Phenol	298	0.920	2.049	0.9957	0.190	2.213	0.9793
	313	0.703	1.908	0.9969	0.336	1.467	0.9767
p-Nitrophenol	298	1.845	2.752	0.9977	0.377	1.014	0.9867

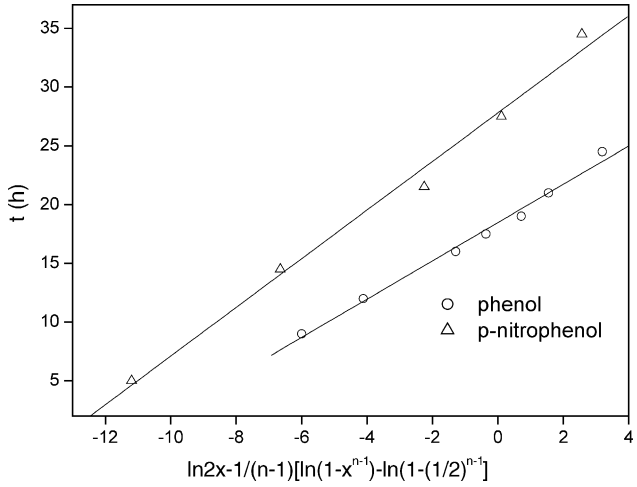

Fig. 2. Validity of the model based on the constant-pattern wave approach theory and the Freundlich model (T = 298 K, U_0 = 34.9 cm/h, C_F = 5.32 mmol/L, L = 5.71 cm, L/R = 3.88, 3 g resin).

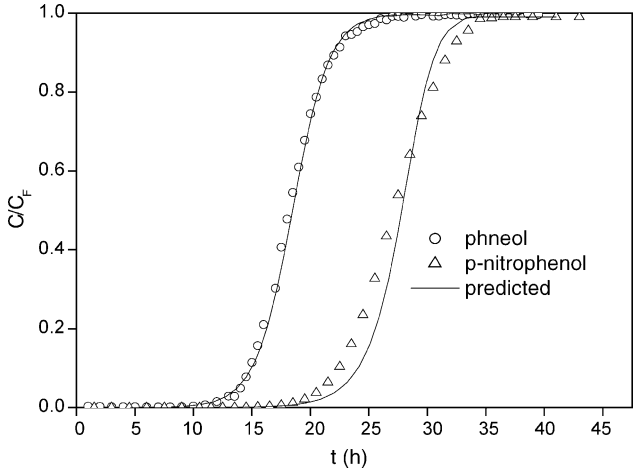

Fig. 3. Breakthrough curves of phenol and *p*-nitrophenol adsorption onto resin NDA-100 (T = 298 K, U_0 = 34.9 cm/h, C_F = 5.32 mmol/L, L = 5.71 cm, L/R = 3.88, 3 g resin).

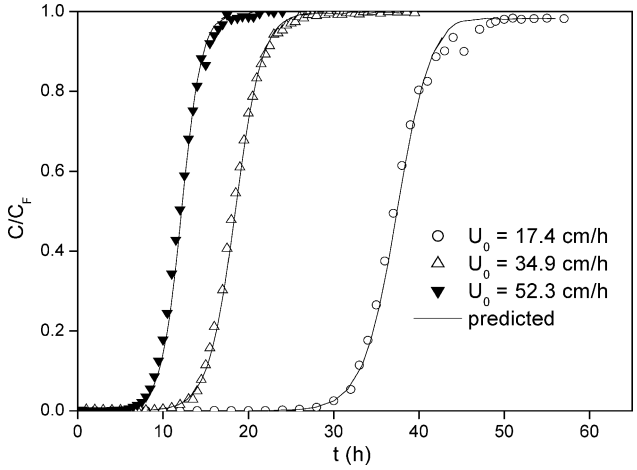

Fig. 4. Effect of feed flow rate on the breakthrough curve of phenol adsorption onto resin NDA-100 (T = 298 K, C_F = 5.32 mmol/L, L = 5.71 cm, L/R = 3.88, 3 g resin).

4.3. Effect of feed flow rate and feed concentration

Figs. 4 and 5 show the breakthrough curves at different feed flow rate. The influence of feed flow rate on the half breakthrough time ($t_{1/2}$) and $K_L a$ is shown in Figs. 6 and 7, indicating a good linear dependence. $t_{1/2}$ decreases and $K_L a$ increases with increasing feed flow rate, which is consistent with conclusion that $K_L a$ varied linearly with the feed flow rate [18].

Fig. 8 shows the breakthrough curves at different feed concentrations. The $t_{1/2}$ values decrease with increasing C_F, on the other hand, $K_L a$ increases slightly with increasing C_F. This means the breakthrough curve is steeper at higher C_F. It is likely that the driving force of mass-transfer in the liquid-film is enhanced when C_F increased. Su-Hsia Lin et al. also found the similar tendency while studying column adsorption of acid dye onto pristine and acid-activated clays [25]. The

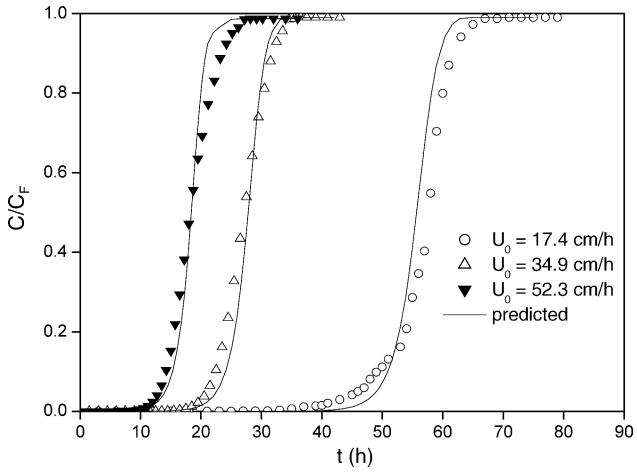

Fig. 5. Effect of feed flow rate on the breakthrough curve of *p*-nitrophenol adsorption onto resin NDA-100 (T = 298 K, C_F = 5.32 mmol/L, L = 5.71 cm, L/R = 3.88, 3 g resin).

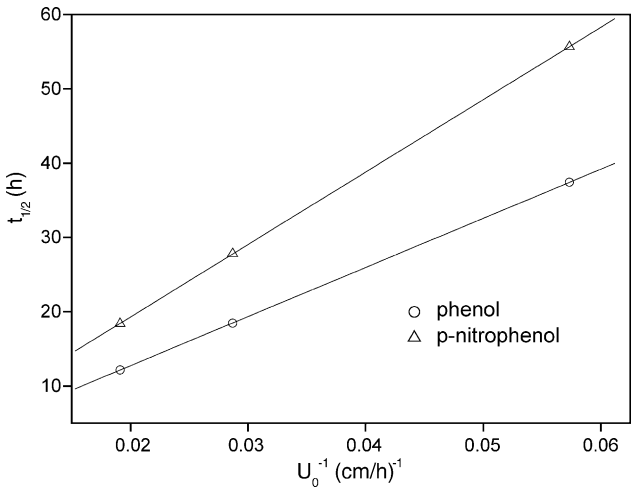

Fig. 6. Effect of feed flow rate on the breakthrough half time $t_{1/2}$ (T = 298 K, C_F = 5.32 mmol/L, L = 5.71 cm, L/R = 3.88, 3 g resin, U_0 = 17.4, 34.9 and 52.3 cm/h, respectively).

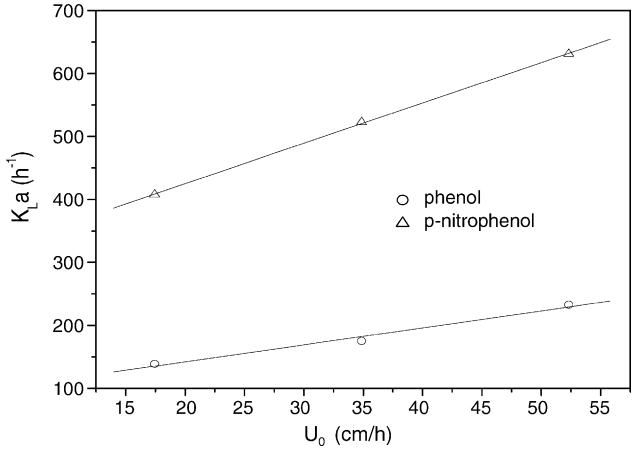

Fig. 7. Effect of feed flow rate on the volumetric liquid-phase coefficients $K_L a$ (T = 298 K, C_F = 5.32 mmol/L, L = 5.71 cm, L/R = 3.88, 3 g resin, U_0 = 17.4, 34.9 and 52.3 cm/h, respectively).

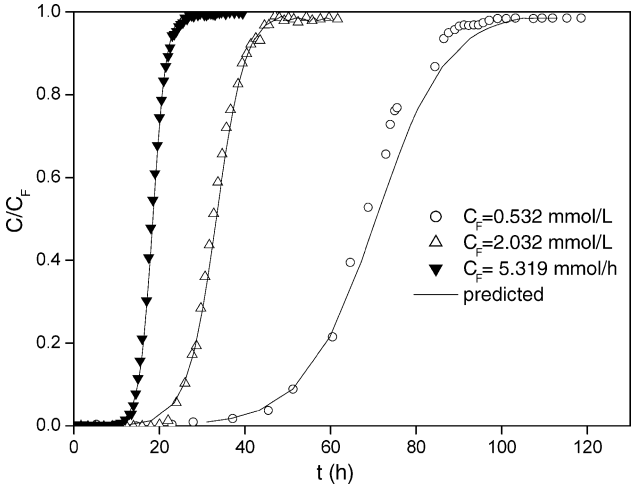

Fig. 8. Effect of feed concentration on the breakthrough curve of phenol adsorption onto resin NDA-100 (T = 298 K, U_0 = 34.9 cm/h, L = 5.71 cm, L/R = 3.88, 3 g resin).

distribution of solute adsorbed in the resin may be determined by intraparticle diffusion rate of the solute into the matrix, which depends on the concentration gradient of solute and the resin porosity. When the C_F increases, the higher initial flux results in the solute shooting deep into the interior matrix [26], and the adsorption sites within the micropore of resin could be occupied adequately, which leads to the higher adsorption capacity at larger C_F.

4.4. Effect of bed height, temperature and aspect ratio

As shown in Fig. 9, the $t_{1/2}$ value is roughly proportional to the bed height at a given U_0. On the other hand, increasing bed height has little effect on the $K_L a$. This observation agrees with previous result for the sorption of phenols onto surfactant-modified montmorillonite in column systems [19].

The effect of the temperature and aspect ratio on the experimental and predicted breakthrough curves is shown in Figs. 10 and 11, respectively. The values of $t_{1/2}$ and $K_L a$ decrease with increasing temperature because the adsorption of phenols onto resin NDA-100 can be considered as physical adsorption, and the adsorption capacity decreases with increasing temperature [27]. Different aspect ratios at given amount of resin adsorbent have little effect on the breakthrough curves in the current study (Fig. 11), indicating that a too large value of aspect ratio is not essential when designing adsorption process in field application.

Many correlations were developed to express the Sherwood number as a function of the Reynolds number and Schmidt number, among of which the following one always gives a satisfactory prediction of the individual liquid-film mass-transfer coefficient in column adsorption experiment [28]:

$$\mathrm{Sh} = (2 + 0.644\mathrm{Re}^{1/2}\mathrm{Sc}^{1/3})[1 + 1.5(1 - \varepsilon)] \quad (18)$$

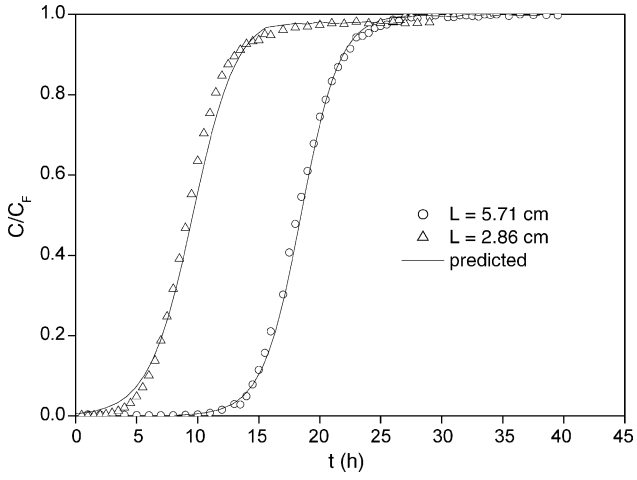

Fig. 9. Effect of bed height on the breakthrough curve of phenol adsorption onto resin NDA-100 (T = 298 K, U_0 = 34.9 cm/h, C_F = 5.32 mmol/L, L/R = 3.88, 3 g resin).

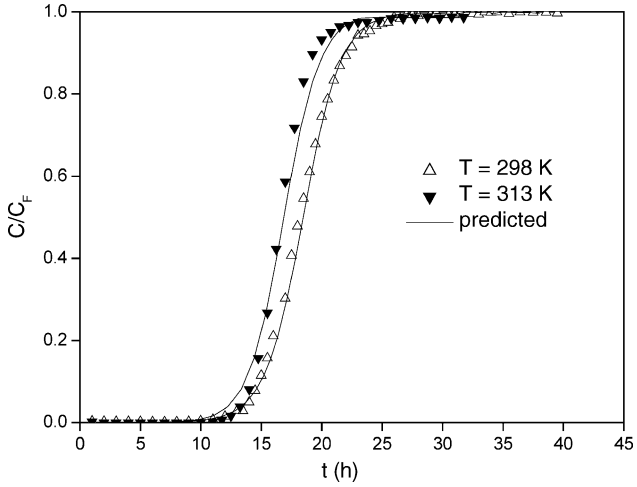

Fig. 10. Effect of temperature on the breakthrough curve of phenol adsorption onto resin NDA-100 (U_0 = 34.9 cm/h, C_F = 5.32 mmol/L, L = 5.71 cm, L/R = 3.88, 3 g resin).

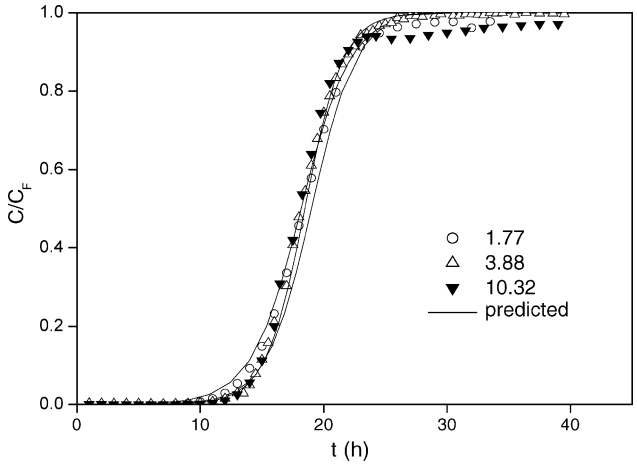

Fig. 11. Effect of aspect ratio on the breakthrough curve of phenol adsorption onto resin NDA-100 (T = 298 K, Q = 60mL/h, C_F = 5.32 mmol/L, 3 g resin).

where

$$\mathrm{Sh} = \frac{d_p k_L}{D} \quad \mathrm{Re} = \frac{\rho_L u_0 \varepsilon d_p}{D} \quad \mathrm{Sc} = \frac{\mu}{\rho_L D}$$

Determining k_L from Eq. (18) and calculating the mass-transfer area per unit bed volume by $a = 6(1 - \varepsilon)/d_p$, we found that the volumetric mass-transfer coefficients based on the liquid-film diffusion model are higher than those from the experimental breakthrough curves. For example, the calculated $k_L a$ is equal to 208.3 h^{-1} for column test run 3 while the experimental $K_L a$ is 163.8 h^{-1}. It implies that the solid-phase mass-transfer resistance does exist and play a certain role in the breakthrough curve.

5. Conclusions

A model based on the constant-pattern wave approach theory and the Freundlich model was used to predict the

breakthrough curves of phenol and *p*-nitrophenol adsorption onto resin NDA-100 at different test conditions. Batch column runs indicate it would predict the breakthrough curves satisfactorily.

Two important parameters ($t_{1/2}$ and $K_L a$) in the above-mentioned model can be directly read from the intercept and slope of the $[\ln 2x - (1/n-1)\ln(1-x^{n-1}/1-(2)^{1-n})]$ versus t curve, and they are related directly to the operating parameters such as the feed flow rate, feed concentration, temperature and bed height. It can be observed that the value of $K_L a$ increases and $t_{1/2}$ decreases linearly with the feed flow rate, and $t_{1/2}$ is roughly proportional to the bed height while $K_L a$ would keep identical.

References

[1] Q.L. Zhang, K.T. Chuang, Adsorption of organic pollutants from effluents of a Kraft pulp mill on activated carbon and polymer resin, Adv. Environ. Res. 5 (2001) 251–258.

[2] S. Rengaraj, K.H. Yeon, Removal of chromium from water and wastewater by ion exchange resins, J. Hazard. Mater. 87 (2001) 273–287.

[3] C.A. Grande, M. Otero, Adsorption of salicylic acid onto polymeric adsorbents and activated charcoal, React. Funct. Polym. 60 (2004) 203–213.

[4] S. Karcher, A. Kornmüller, Anion exchange resins for removal of reactive dyes from textile wastewaters, Water Res. 36 (2002) 4717–4724.

[5] Z.Y. Xu, Q.X. Zhang, et al., Adsorption of naphthalene derivatives on different macroporous polymeric adsorbents, Chemosphere 35 (1997) 2269–2276.

[6] S.H. Lin, C.Y. Huang, Adsorption of BTEX from aqueous solution by macroreticular resins, J. Hazard. Mater. A 70 (1999) 21–37.

[7] M. Lehmann, A.I. Zouboulis, Modeling the sorption of metals from aqueous solutions on goethite fixed-bed, Environ. Pollut. 113 (2001) 121–128.

[8] G.H. Xiu, P. Li, Prediction of breakthrough curves for adsorption of lead (II) on activated carbon fibers in a fixed bed, Carbon 38 (2000) 975–981.

[9] W.T. Tsai, C.Y. Chang, Adsorption properties and breakthrough model of 1,1-dichloro-1-fluoroethane on activated carbons, J. Hazard. Mater. 69 (1999) 53–66.

[10] D. Chatzopoulos, A. Varma, Aqueous-phase adsorption and desorption of toluene in activated carbon fixed beds: experiments and model, Chem. Eng. Sci. 50 (1995) 127–141.

[11] A.J. Slaney, R. Bhamidimarri, Adsorption of pentachlorophenol (PCP) by activated carbon in fixed beds: application of homogeneous surface diffusion model, Water Sci. Technol. 38 (1998) 227–235.

[12] A. Wolborska, P. pustelnik, A simple method for determination of the breakthrough time of an adsorption layer, Water Res. 30 (1996) 2643–2650.

[13] Z.Y. Xu, Q.X. Zhang, et al., Applications of porous resin sorbents in industrial wastewater treatment and resource recovery, Crit. Rev. Environ. Sci. Technol. 33 (2003) 363–389.

[14] R.X. Wei, J.L. Chen, et al., Study of adsorption of lipoic acid on three types of resin, React. Funct. Polym. 59 (2004) 243–252.

[15] P. Kanekar, S. Sarnaik, Microbial technology for management of phenol bearing dyestuff wastewater, Water Sci. Technol. 33 (1996) 47–51.

[16] A.D. Annibale, R. Casa, Lentinula edodes removes phenols from olive-mill wastewater: impact on durum wheat (Triticum durum Desf.) germinability, Chemosphere 54 (2004) 887–894.

[17] G.I. García, P.R. Jiménez Peña, Removal of phenol compounds from olive mill wastewater using *Phanerochaete chrysosporium*, *Aspergillus niger*, *Aspergillus terreus* and *Geotrichum candidum*, Process Biochem. 35 (2000) 751–758.

[18] J.M. Chern, Y.W. Chien, Adsorption of nitrophenol onto activated carbon: isotherms and breakthrough curves, Water Res. 36 (2002) 647–655.

[19] R.S. Juang, S.H. Lin, Sorption of phenols from water in column systems using surfactant-modified montmorillonite, J. Colloid Interf. Sci. 269 (2004) 46–52.

[20] Z.H. Ye, Base of Sorption Separation Process, Chemistry Industry Press, Beijing, 1988.

[21] T. Sherwood, R. Pigford, Mass Transfer, McGraw-Hill, NewYork, 1975.

[22] J.M. Chern, S.N. Huang, Study of non-linear wave propagation theory. 1. Dye adsorption by activated carbon, Ind. Eng. Chem. Res. 37 (1998) 253–257.

[23] B.C. Pan, Y. Xiong, et al., Adsorption of aromatic acids on an aminated hypercrosslinked macroporous polyer, React. Funct. Polym. 53 (2002) 63–72.

[24] A.M. Li, Q.X. Zhang, et al., Adsorption of compounds from aqueous solution by a water-compatible hypercrosslinked polymeric adsorbent, Chemosphere 47 (2002) 981–989.

[25] S.H. Lin, R.S. Juang, Adsorption of acid dye from water onto pristine and acid-activated clays in fixed beds, J. Hazard. Mater. B 113 (2004) 195–200.

[26] R.S. Juang, J.Y. Shiau, Adsorption isotherms of phenols from water onto macroreticular resins, J. Hazard. Mater. 70 (1999) 171–183.

[27] A.M. Li, Q.X. Zhang, et al., Adsorption of phenolic compounds on Amberlite XAD-4 and its acetylated derivative MX-4, React. Funct. Polym. 49 (2001) 225–233.

[28] P.V. Roberts, P. Cornal, External mass-transfer rate in fixed-bed adsorption, J. Environ. Eng. Div. ASCE 111 (1985) 891–905.